OPEN ACCESS

Review Article

# Numerical simulation and nasal air-conditioning

## Abstract

Heating and humidification of the respiratory air are the main functions of the nasal airways in addition to cleansing and olfaction. Optimal nasal air conditioning is mandatory for an ideal pulmonary gas exchange in order to avoid desiccation and adhesion of the alveolar capillary bed. The complex three-dimensional anatomical structure of the nose makes it impossible to perform detailed in vivo studies on intranasal heating and humidification within the entire nasal airways applying various technical set-ups. The main problem of in vivo temperature and humidity measurements is a poor spatial and time resolution. Therefore, in vivo measurements are feasible only to a restricted extent, solely providing **single** temperature values as the complete nose is not entirely accessible. Therefore, data on the overall performance of the nose are only based on one single measurement within each nasal segment. In vivo measurements within the **entire** nose are not feasible.

These serious technical issues concerning in vivo measurements led to a large number of numerical simulation projects in the last few years providing novel information about the complex functions of the nasal airways. In general, numerical simulations merely calculate predictions in a computational model, e.g. a realistic nose model, depending on the setting of the boundary conditions. Therefore, numerical simulations achieve only **approximations** of a possible real situation.

The aim of this review is the synopsis of the technical expertise on the field of in vivo nasal air conditioning, the novel information of numerical simulations and the current state of knowledge on the influence of nasal and sinus surgery on nasal air conditioning.

**Keywords:** climatisation, air flow, numerical simulation, CFD, nose

**Tilman Keck**[1]
**Jörg Lindemann**[2]

1 Department of Otorhinolaryngology, Head and Neck Surgery, Elisabethinen-Krankenhaus GmbH, Academic Hospital of the University of Graz, Austria

2 Department of Otorhinolaryngology, Head and Neck Surgery, University of Ulm, Germany

## 1 Introduction

The nasal airways have several functions such as the sense of smell, nasal defence, and creation of resistance during expiration for prevention of alveolar collapse. Besides these functions, the nose has special functions during inspiration and expiration. During inspiration, the air is heated, humidified, and cleaned. The so-called "air-conditioning" [1], [2], [3] within the nasal airways should guarantee an undisturbed alveolar gas exchange. During expiration, the nasal airways partially extract heat and humidity from the exhaled air. Thus, the loss of heat and moisture is reduced during respiration. Additionally during expiration, particles that are not retained in the bronchial airways are deposited within the nasal airways [4], [5].

The nasal functions "warming" and "humidification" are called climatisation [6], [7]. Nasal cleaning is described by several terms. "Filtration" means removal of particles from the respiratory air. "Deposition" means removal of particles by sedimentation on the nasal mucosa. "Retention" stands for the retention of mainly gaseous particles of the air. "Clearance" means removal of deposited particles on the mucosa by ciliary activity [8].

Climatisation is mainly fulfilled by the nasal airways. Lower parts of the airways like the oropharynx, the hypopharynx, the larynx, and the trachea only minimally participate in climatisation [9], [10], [11]. Already within the nasopharynx the air temperature reaches approximately 31 to 34 °C with a relative humidity of 90 to 95% [12], [13]. The nasal part in deposition depends on the attributes of the in-streaming particles (hygroscopic or hydrophobic, size, aerodynamic diameter, surface, density, and other chemical variables) [5], [8]. Particles with a diameter between 0.4 and 3.0 µm pass the nasal airways to a great amount and are mainly deposited in the bronchial airways. Particles with a diameter lower than 0.4 µm and bigger than 10 µm are mainly filtered in the nose [5], [14], [15]. Similar to the climatisation function, particle filtration depends on respiratory parameters like breathing frequency and tidal volume [8].

To characterise the climatisation function of the nose, additional explanation of specific terms is necessary. Humidity is a measure of molecular water vapour in a gas. Whereas "absolute humidity" describes the real amount of water in a gas volume (g/m³ or g/kg), "relative humidity" (RH) stands for the amount of humidity in a specific air volume as part of the maximally possible amount of water at a specific air temperature (in %RH). Relative humidity is a parameter of saturation of air with water vapour and depends on the temperature of the air.

Absolute humidity is not temperature dependent. With the so-called "Mollier diagram", calculations of the humidity parameters are possible [16], [17]. The heat content of a gas (enthalpy; KJ/Kg) depends on the temperature (°C), the concentration of water vapour, and the relative humidity. Calculation of the enthalpy needs precise synchronous detection of temperature and relative humidity, similar to calculations of absolute humidity. Enthalpy stands for the amount of energy that is necessary to heat a specific volume of air. It is not regularly calculated during measurements in breathing cycles [17].

# 2 Nasal anatomy and physiology

The nasal cavity is divided in several regions. The intranasal regions from anterior to posterior are: the nasal vestibule; the nasal valve area (bounded by the nasal septum, the lower margin of the upper lateral cartilage, the isthmus nasi, and the head of the inferior turbinate), the anterior turbinate area (area between nasal valve and head of the middle turbinate, inferiorly the inferior turbinate turbinate), the posterior turbinate area (posterior part of the inferior turbinate and choanae), and the nasopharynx [18]. The nasal valve area is the narrowest part of the nose, measuring approximately 40 $mm^2$. The nasal cavity has a cross section area in the anterior and posterior turbinate area up to 150 $mm^2$ [18], [19], [20].
Humans breathe approximately 10,000 to 15,000 litre air per day. The highly vascularised mucosa has a dominant part in climatisation of respired air [21].The surface area of the nasal mucosa is about 100 to 200 $cm^2$ [22], [23]. In the nasal vestibule, the nasal airways are covered with skin and posteriorly with squamous epithelium, partially lined with vibrissae. In the nasal valve region, the nasal lining changes from squamous epithelium to ciliated columnar secretory lining and respiratory epithelium, consisting of ciliated and nonciliated cells, columnar cells with microvilli, goblet cells, and basal cells [21], [24]. The respiratory epithelium is covered by a fluid lining, consisting of a low-viscous basal periciliary fluid (sol phase) and a high-viscous upper mucus (gel phase) [25], [26]. Goblet cells secrete a viscous fluid. The predominating seromucous glandular cells, lying under the basal membrane, secrete a mixed seromucous fluid [25], [27]. The moistening of the mucosa with lacrimal fluid and secretion from the sinuses is quantitatively insignificant [28]. The subepithelial tissue contains arteries, arteriols, venols, capillary vessels, and sinusoids.
The regulation of perfusion of the nasal mucosa is very important for the control and regulation of nasal climatisation. This regulation is effected by resistance vessels that are sympathetically innervated [29], [30]. Resistance vessels as well as capacitance vessels are surrounded by sympathic nerv facicles that are controlled via noradrenalin by α1- und α2-adrenergic receptors [31]. Vasoconstrictives such as alpha-sympathomimetics (e.g. the imidazol-derivative xylometazolin) predominantly act as alpha-2-receptoragonists leading to a gradual reduction of the blood flow after topical application [32].In addition, many neuropeptides and mediators affect the perfusion of the nasal mucosa [33].
The supply of heat and humidity from the nasal mucosa to the inspiratory air leads to an alteration of the nasal mucosal temperature. While inspiration decreases the nasal mucosal temperature, expiration leads to a reheating of the mucosa [34], [35], [36].
The airflow characteristics of the inhaled and exhaled air within the nasal cavity are crucial for the respiratory function. Respiration at rest accelerates the inhaled air to a speed of up to 18 m/s near to the nasal valve. Within the posterior part of the nose the air velocity decelerates to 2–3 m/s [37]. During inspiration, the air flow is diverged in the nasal valve region, whose concave shape disperses the air all over the surface of the turbinates within the middle and posterior regions of the nose [38]. During expiration, the turbulent airflow within the middle and posterior nasal regions are aligned and become laminar upon passing the nasal valve region [37], [39], [40].
The dispersion of the inhaled air all over the surface of the turbinates leads to a close contact between the surface of the humid nasal mucosa and the air allowing a sufficient air conditioning and deposition of particles. The nasal airway resistance may not be too high to prevent mouth breathing, which is considerably less favourable for the climatisation of the inhaled air. Abnormally low airway resistance lead to excessively high air passage with concomitantly shorter contact times between air and mucosa resulting in an insufficient air conditioning.

# 3 Experimental measurement techniques

## 3.1 Temperature measurements

The experiments of Webb et al. and Keck et al. [41]; [42], [43] involved the use of a copper-constantan thermocouple for intranasal temperature measurements, e.g. under cold external conditions in Alaska [41]. A thermocouple is a junction between two different metals, located at the tip of the sensor producing a temperature-dependent voltage. In contrast, Cole used a so called type U-Thermistor or platinum thermometer for his studies [9], [10], [34], [44]. These sensors use the temperature dependence of the resistance for measuring the temperature. McFadden performed temperature measurements within the trachea and the bronchia by means of a thermistor [45].
More recently, thermographic cameras (so-called infrared cameras) are used to study the endonasal temperature and the heat exchange between air and mucosa [46], [47].

## 3.2 Humidity measurements

For the first time, Liese et al. achieved short response times for measurements of the humidity by using a mass spectrometer without simultaneously recording the temperature [48]. Drettner et al. also used a mass spectrometer coupled to a catheter placed within the nasopharynx [49], [50]. By means of a mass spectrometer water molecules in the air can be directly identified. For that propose, the air is guided through electric and magnetic fields. Depending on their deflection the water molecules impinge on different locations on an ion detector. This induces an electric current being proportional to the number of the water molecules.

## 3.3 Simultaneous measurements of temperature and humidity

Perwitzschky used in early studies a mercury thermometer and calcium chloride as humidity adsorbent to measure humidity within the nasopharynx of volunteers [51], [52]. Calcium chloride is a hygroscopic salt that gains weight by absorption of water. The absorbed amount of water was calculated by the weight difference before and after humidity measurement. Seeley used a copper-constantan thermocouple to measure the temperature at three different places within the nose. In his studies the humidity was determined with magnesium perchlorate as water absorbent [53]. A high amount of investigations were reported by Ingelstedt, who used a konstantan-nickel-chromium thermocouple and a mercury psychrometer [3], [11], [12]. The applied psychrometer consisted of two thermocouples. One of the thermocouples was covered by a wet blanket that cooled via evaporation in dry air. The temperature difference between these two thermocouples was reflecting the actual degree of humidity of the air.
Primiano. et al. constructed a suction catheter connected to a thermistor and a mass spectrometer for intranasal positioning. Clinical data were not collected using this experimental device [54], [55].
Rouadi et al. and Keck et al. developed an experimental setup consisting of a capacitive humidity sensor for detection of relative humidity and a thermistor or respectively a thermocouple [13], [42]. Several working groups in the field of anaesthesia also used experimental set-ups applying a capacitive humidity sensors in breathing circuits [56], [57], [58]. Kaufman et al. developed several thermoelements within a tube for temperature recording in the air and on the mucosa. Measurements were performed within the oral cavity and calculations of humidity coefficients were done [59].
In summary, mainly mercury thermometers, thermocouples and thermistors were used for nasal temperature recording. The fastest response times have thermocouples. Humidity measurements were performed using gravimetric, psychrometric, mass spectrometric, and capacitive sensor technology. The highest experience is available using capacitive sensors and mass spectrometers (Table 1).

# 4 Nasal air conditioning

## 4.1 In vivo measurements in humans

Detection systems for air-conditioning should present the following characteristics: simple, precise, fast response time, good clinically applicable in vivo.
The devices should be of comfortable for the patients or volunteers and easy to handle in the clinical daily routine. The applied sensors should be as small as possible to avoid irritations of the mucosa due to contact.
One problem in intranasal measurements of air conditioning is that only regional data of climatic conditions within the nasal airways are available and feasible. It would be preferable to detect how a defined “portion of inhaled air” is climatically changed during its nasal passage. This is currently not feasible due to technological and anatomical reasons.
Intranasal positioning of a temperature probe within the nose is usually not problematic. The air temperature can be detected by using commercially available thermometers with a response time of 0.1 s in streaming air [42]. Longer response times were measured in earlier experiments [35], [41], [50], [60]. However, temperature measurements during the respiratory cycle were performed with these slow-reacting devices as well.
In former times used mass spectrometers [48], [50], [54], [55], [61] showed faster response times than capacitive humidity sensors recently used [13], [43], [62], [63]. However, mass spectrometers were not widely used as they were not easy to handle and the long suction systems with high amount of condensation biased the measurement results. A experimental infrared hygrometer presented an even faster response time compared to capacitive humidity sensors or mass spectrometers [64]. Yet, no physiological in vivo data are reported.
Mass spectrometers have the basic advantage to directly measure absolute humidity, in contrast to capacitive relative humidity sensors. However, even the use of a heating map around the suction system does not sufficiently avoid condensation [65].

## 4.2 Nasal air conditioning in humans

In a group of 50 healthy subjects, end-inspiratory airway temperature significantly increased within the anterior part of the nasal airways, e.g. close to the nasal valve area and anterior turbinate area [43]. The nasopharyngeal temperature was approximately 34 °C according to results of different working groups [13], [41], [66]. The air temperature within the nasopharynx is close to the temperature of the nasal mucosa [36], [67]. Similar temperature measurements with low end-inspiratory and high end-expiratory values were also performed by Webb [41] and Cole [9].

**Table 1: Temperature and humidity measurements: methods and results**

| Working group | Year | Method | Results |
|---|---|---|---|
| Perwitzschky [51, 52] | 1928, 1930 | Mercury thermometer, moisture absorbens | 32℃ and 80% RH in the nasopharynx. No influence of cocaine on nasal air-conditioning. |
| Seeley [53] | 1940 | Thermoelement, moisture absorbens | High air temperatures in the choanae. |
| Webb [41] | 1951 | Thermoelement | High heating capacity of the nose during respiration of very cold air (Alaska). |
| Cole [9, 10, 34, 44] | 1953, 1954 | Thermistor | Blood flow of the nasal mucosa of minor importance for nasal climatisation. Influence of vasodilators on nasal mucosal temperature. |
| Ingelstedt et al. [11, 12] | 1949, 1951, 1956 | Thermoelement, Psychrometer | Subglottic air: appr. 36℃ and almost saturated with water vapour after inspiration. Influence of atropine on nasal humidity via parasympathic innervation of nasal glands. |
| Liese et al. [48] | 1973 | Mass spectrometer | Low influence of nasal mucosa on nasal moisturising capacity (max. 10%). |
| Drettner et al. [49, 50] | 1977, 1981 | Mass spectrometer | Basics of nasal detection systems. |
| Primiano et al. [54, 55] | 1984, 1988 | Thermistor, Mass spectrometer | No clinical data presented. |
| McFadden et al. [45] | 1985 | Thermistor | Influence of breathing rate on tracheal temperature. Special importance of lower airways on air-conditioning of inhaled air. |
| Rouadi et al. [13] | 1999 | Thermistor, capacitive humidity sensor | Respiration of cold dry air reduces air temperature and the amount of water vapour, while relative humidity keeps constant in the nasopharynx. |
| Keck et al. [42] | 2000 | Thermoelement, capacitive humidity sensor | Increase of temperature and humidity in the anterior part of the nasal airways. |
| Kaufman et al. [59] | 2006 | Multiple Thermoelements | Measurement and calculation of heat and humidity coefficients in the oral cavity. |

The increase of temperature and humidity within the nasal airways is almost synchronous [42]. Humidity also increases significantly within the anterior third of the nose (Figure 1, Figure 2).

Webb found a pharyngeal temperature of approximately 29 °C with an ambient air temperature of 7 °C [41]. The contact time of inspired air with the surrounding mucosa of the anterior segment of the nose seems to be sufficient enough to warm the inspired air although the air stream has a high velocity in this part of the nose [68]. Heating of air significantly depends on the high inspiratory and expiratory temperature gradient within the anterior segment of the nasal airways. Mixture of inhaled relatively colder air with expired relatively warmer air in the anterior nasal segment is also of importance for nasal heating.

It is still unclear if the nasal mucosa can warm air without circulating, but resting air. During expiration, airway temperature only decreases minimally in direction from the nasopharynx to the nasal vestibule and still is approximately 34 °C at the nasal valve area at the end of expiration [69]. This is in accordance to the results of Cole and Webb [9], [41]. At the end of inspiration, the air temperature quickly increases during rest of breathing. These results demonstrate heat transfer from the mucosa to the air occurs even during rest of breathing [70]. For achieving this, the nasal mucosa needs a high potential of factors increasing the mucosal blood supply to com-

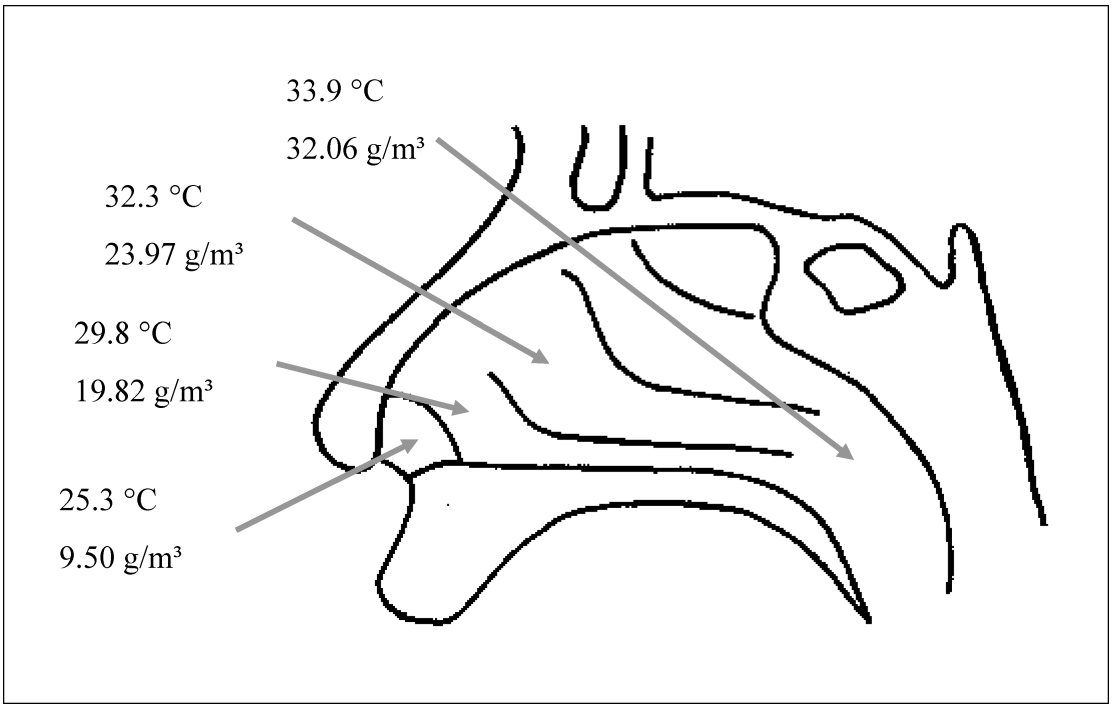


**Figure 1: Increase of air temperature and absolute humidity during inspiration of air (25 °C; 8.06 g Wasser/m³).**

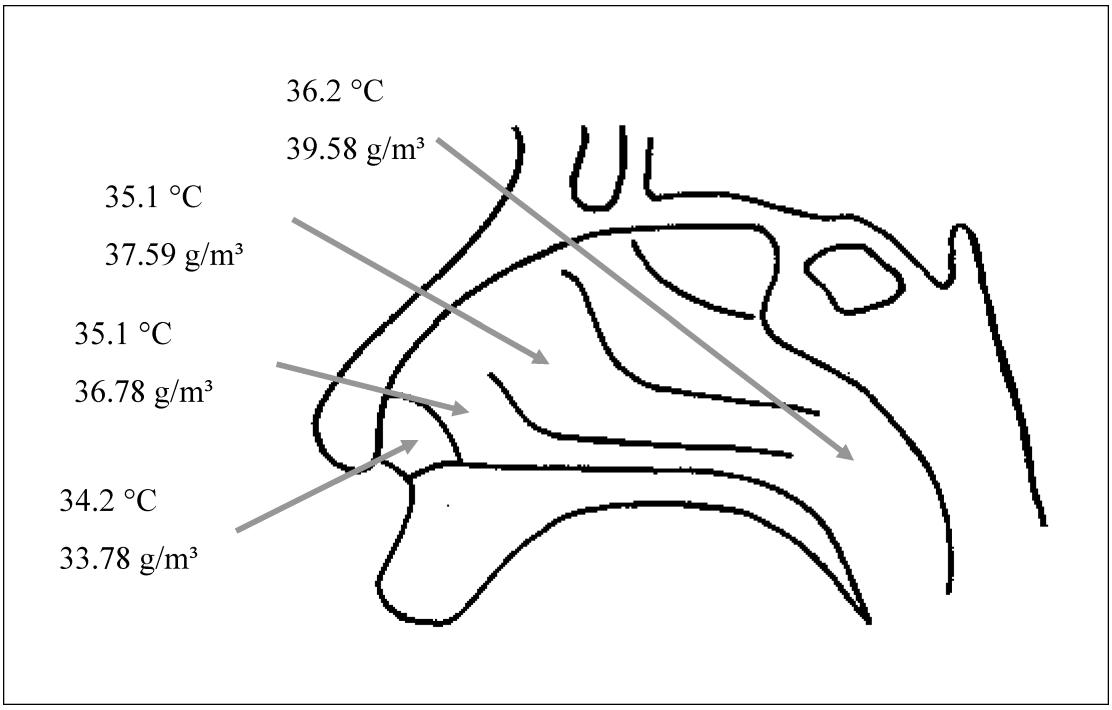


**Figure 2: Decrease of air temperature and absolute humidity during expiration.**

pensate cooling at the mucosal surface and to warm the surrounding air. Without this particular warming capacity, mucociliary clearance being highly dependent on the airway temperature would be impaired and reduced viscoelasticity of the mucosal surface and decreased nasal particle deposition would occur [71], [72], [73].

In simultaneous measurements of temperature and relative humidity, a high increase of relative humidity in the anterior nasal segment could be detected. The end-inspiratory nasopharyngeal relative humidity reached approximately 90%. However, nasal humidification is not yet finished at this level. The end-inspiratory nasopharyngeal temperature is approximately 34 °C. Further warming up to 37 °C occurs within the lower airways. Further warming of air is accompanied by an exponential elevation of maximal transport capacity of air for water vapour [16], [17] resulting in a complete saturation of air with water vapour in the bronchial airways [3]. Warming of air within the anterior segment of the nose is the precondition for further increase of enthalpy in the middle and posterior nasal airways [70]. During the nasal passage the air stream within the nasal valve area increases further ele-

vation of saturation of air with water vapour due to a more turbulent airflow [38].

Small seromucous glands located in the anterior part of the nasal septum and the turbinates are feasible donors of humidity. Until now, it is still unclear how the serous glands of the nasal vestibule and the nasal valve area relevantly participate in nasal humidification.

A short-term exposure to cold dry air or warm humid air does not impair nasal warming of normal ambient air. Humidification of ambient air after a short-term exposure to cold dry air is impaired, whereas humidification after a short-term exposure to warm humid air is elevated. This phenomenon was detected within the nasal valve area, but not in the anterior turbinate area [74]. A possible explanation could be a reduced mucosal perfusion [75], altered air stream characteristics [76], or changed composition of nasal secretions [77], [78] after cold air exposure with a reduced humidification during breathing relatively warmer air after end of exposure.

Little is known about air conditioning in patients with perennial allergic rhinitis. Rozsasi et al. [79] investigated the effect of nasal antigen challenge in patients with an allgery against house dust mites on nasal air conditioning in correlation to nasal patency and geometry. After nasal allergen challenge with allergen extracts from house dust mites a significant increase in absolute humidity of the intranasal air on the provoked nasal side compared to the unprovoked one could be observed. The authors hypothetically conclude that the increase of the mucosal humidity resulting from the nasal allergen challenge is responsible for an increase in nasal air conditioning capacity as no correlation to changes in nasal perimeter and patency was found.

Heating and moistening of the air are very closely related. The temperature difference between the nasal mucosal surface and the respiratory air during inspiration and expiration is a prerequisite for heat exchange and humidity exchange between the mucosa and air [35].

Several investigations demonstrated that in vivo measurements of nasal mucosal temperature are variously practicable [67], [80], [81], [82], [83], [84], [85], [86].

There is a great lack of information in the literature about the precise site of detection and the exact time of detection within the respiratory cycle in the published data of nasal mucosal temperature, although the mucosal temperature depends on these two statements [82]. In the literature, nasal temperature has been estimated to run from 30 °C to 36.6 °C [82].

Willatt et al. reported the septal mucosal temperature as measured by infrared thermometry to range from 30.4 °C during inspiration to 32.0 °C during expiration without giving information about the exact intranasal detection site [86]. Fabricant [80] recorded temperature values between 29.7 °C and 34.7 °C in the nose and 32.2 °C and 35.6 °C in the pharynx with a fluctuation during respiration also without data of the precise detection site. Jun and Qingping [81] measured a surface temperature of the anterior mucosa of the inferior nasal turbinate before deep puncture at three points in the nasal region as 26.9 °C before and 27.4 °C after treatment without discussing respiration. Assanasen et al. [67] found a significant increase in nasal mucosal temperature at the anterior portion of the septum over the baseline of 1.9 °C after warming the feet in 42 °C warm water without reporting about the time of detection within the respiratory cycle. Molony et al. [85] investigated the effect of prone posture on nasal septal temperatures in children by means of an infrared thermometry while holding breath without information about the exact intranasal detection site. Mean temperatures in prone position (34.5 °C) were significantly higher compared to the upright position (36.0 °C).

It might be possible that the published results of nasal mucosal temperature are based on changes in the detection site and time of detection within the single study, especially when results show variations in temperature as small as 1 to 2 °C.

The thermocouple (as above mentioned) [42], [43] allowed mucosal temperature recording at defined different detection sites within the nasal cavity without interruption of nasal breathing and irritation of the nasal mucosa [82], [83], [84].

This can not be achieved by the commonly used infrared thermometers for non-contact measurements of the mucosal temperatureas these thermometers do not allow breathing synchronic measurements due to a too long actual response time.

The mean mucosal temperature as measured by the thermocouple described ranges from 30.2 °C at the end of inspiration to 34.4 °C at the end of expiration [82] depending on the point of time within the respiratory cycle and the exact intranasal detection site.

During inspiration, the warmer nasal wall heats the cooler air, during expiration the colder wall cools down the warmer air. This temperature gradient between mucosal surface and inspiratory and expiratory air is essential for an effective heat and water transfer. There is also a close relationship between nasal airflow patterns and nasal mucosal temperature. In regions of turbulent airflow, temperature changes are more pronounced compared to regions of laminar airflow [82]. This fact again confirms the close relation between airflow and intranasal temperature changes. This fact is of particular importance within the anterior nasal segment including the nasal valve area (NVA). Due to airflow turbulences within the NVA, the decrease in mucosal temperature during inspiration is more intense within this area compared to the nasal vestibule and the nasopharynx [82].

Like other body parts and organs, the nose changes as the body ages. Elderly patients frequently complain about the feeling of a dry nose and recurrent crusting probably due to age-related degenerative effects of the nasal mucosa.

For the first time, Lindemann et al. [87] presented a study assessing intranasal air conditioning in relation to age. Intranasal heating and humidification of respiratory air in elderly subjects were compared to a younger control group. Temperature and humidity values were significantly

lower in the elderly study group compared to the younger control group. The minimal cross-sectional areas and volumes measured by acoustic rhinometry were significantly larger in the elderly study group. Nasal complaints in elderly patients are a consequence of lower intranasal air temperature and humidity values combined with relatively enlarged nasal cavities due to involution atrophy of the nasal mucosa.
In summary, there is a significant increase in air temperature and humidity within the anterior nasal segment at the nasal valve level during inspiration. The temperature of the inhaled air increases almost synchronously to intranasal humidity. The temperature gradient between nasal mucosal surface and air is an elementary prerequisite for an efficient heat and moisture exchange. Additionally, the nasal valve area, including the anterior head of the inferior turbinate, plays a crucial role in nasal air conditioning. There is a close relationship between nasal airflow patterns and air conditioning. In regions of turbulent airflow with low flow velocities temperature and humidity changes are more pronounced compared to regions of laminar airflow.

## 4.3 Numerical simulations

The complex 3-D structure and poor accessibility of the nasal cavity have prevented detailed in vivo studies of nasal air conditioning. Therefore, in vivo measurements (temperature, humidity, filtration of particles) within the centre of the nasal air stream with the above mentioned measurement techniques are feasible only to a certain extent. Basically, values had only been recorded within the region of the nasal nostrils or within the nasopharynx. Investigations at different, precisely defined intranasal detection sites representing regional differences and the intranasal mapping are rare.
The main problem of in vivo measurements of nasal air conditioning is a poor spatial and time resolution. Due to the complex anatomical structure of the nasal cavity, in vivo measurements within the entire human nose are technically not realizable. Therefore, in vivo measurements are feasible only to a certain extent, providing solely single values as the nose is not entirely accessible. Data on the overall performance based on only one single measurement within each nasal segment are available. In order to obtain in vivo temperature and humidity plots, infinite single measurements during the respiratory cycle would be necessary. Therefore, in vivo measurements cannot provide a precise mapping of the intranasal temperature and humidity distribution necessary to identify the actual contribution of each nasal segment.
Additionally, in vivo studies on intranasal airflow patterns are technically not realizable even though airflow patterns are indispensable for optimal intranasal air conditioning. In order to solve these problems of in vivo measurements, numerical simulations applying computational fluid dynamics (CFD) offer new techniques to analyse nasal air conditioning together with airflow patterns.

### 4.3.1 Simulation of intranasal air flow

Nasal airflow is essential for an adequate intranasal climate. In vivo studies of intranasal airflow patterns are prevented due to the complex structure of the nose. Therefore, a variety of experimental and numerical models have been used for the analysis of airflow patterns.
In fluid dynamics experiments, nose-like models had been applied in numerous studies [88], [89], [90], [91], [92], [93], [94], [95], [96], [97], [98], [99], [100], [101], [102]. Nowadays, numerical models for airflow simulation play an increasingly important role. Numerical simulation is a method displaying a real environment, in our case the human nose, within a computational model. Computational fluid dynamics (CFD) is a numerical simulation application to study various flow dynamics. It is a well established method employed in aircraft manufacturing and the automotive industry. In general, a computational model of the system being represented is generated. The appropriate fluid flow physics are applied to the virtual model, in the case of the human nose a realistic 3-D computational nose model, resulting in a prediction of the fluid dynamics. It allows for displaying and analyzing airflow patterns within the entire human nose in a realistic virtual 3-D model. To provide an anatomically accurate lifelike model of the human nose the models are reconstructed using computed tomography (CT) scans of the nasal cavity (Figure 3).
CFD simulations are applied to study airflow dynamics within the nasal cavity [39], [103], [104], [105], [106], [107], [108], [109], [110], [111], [112], [113], [114], [115], [116], [117], [118], [119], [120], [121], [122], [123], the human upper respiratory tract [124], [125] and the lung [126], [127], [128], [129].
The simulations are based on the numerical solution of the Navier-Stokes equation, representing the general equation for 3-D flow of incompressible and viscous fluids. The numerical solution of the Navier-Stokes equation is the most popular method in CFD. Given the Navier-Stokes equation and a set of suitable boundary conditions it is possible to solve on a grid using the standard numerical techniques. Turbulence models are applied to predict the effects of turbulence within fluid flow without resolving all scales of the smallest turbulent fluctuations.
The results of numerical simulation displaying intranasal airflow patterns complied very well with experimental and rhinoresistometric findings [120], [122].
The existing experimental and numerical studies examining **only** intranasal airflow patterns very often employed unilateral models of either the right or the left nasal cavity. These simulations of intranasal nasal airflow patterns did not provide any information about intranasal heating and humidification of air during respiration.
For the first time, the study group around Lindemann et al. [111], [112], [113], [114], [115], [116] performed CFD simulations of the intranasal air temperature **and** airflow patterns.
Numerical simulations applying CFD offer an analysis and visualisation of airflow patterns within the entire nasal

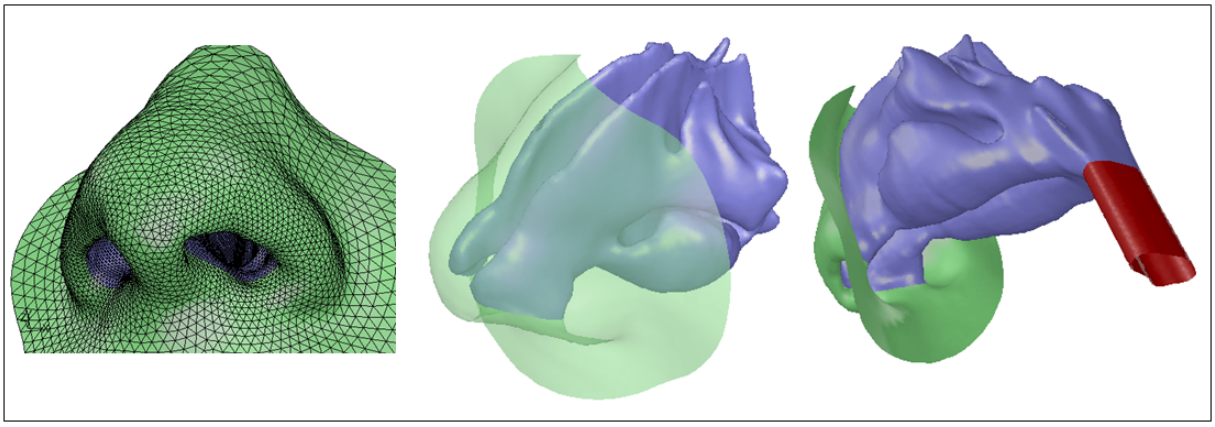

Figure 3: Exemplary three-dimensional model of the human nose used for numerical simulation from different point of views.

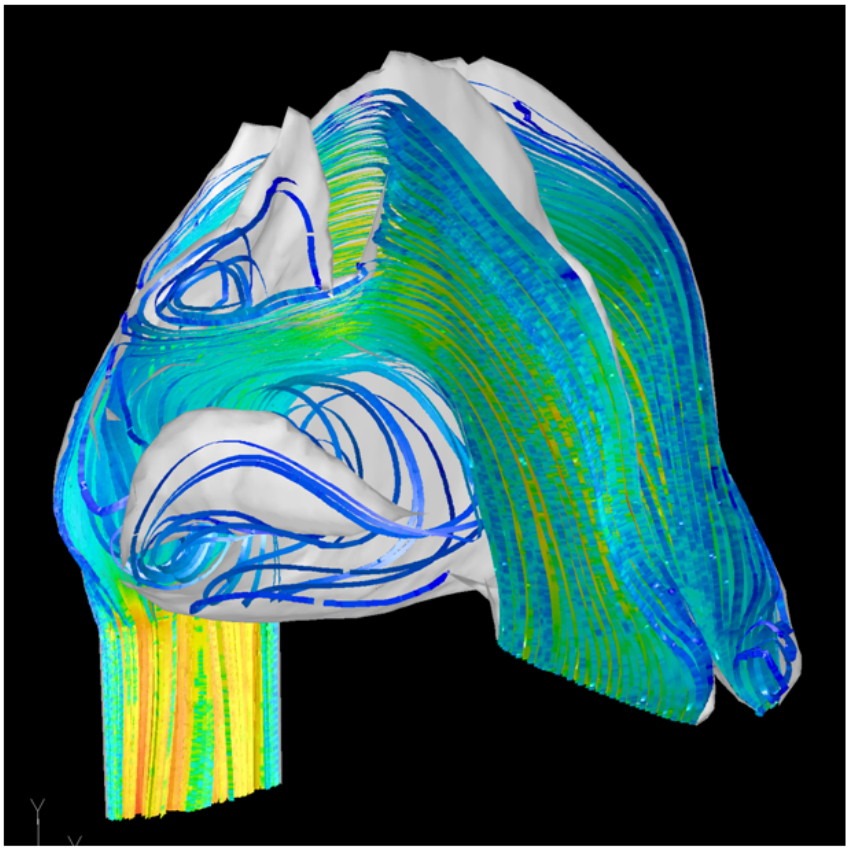

Figure 4: Airflow patterns displayed by path lines within a computational model of a healthy nose during inspiration.

cavity during inspiration and expiration. Variations of airflow patterns like turbulences, vortices, velocity of flow, volume flow, pressure conditions, distribution pattern **and** path lines can be investigated.

The anterior nasal segment, including the nasal valve area (NVA) representing the narrowest segment of the nasal cavity, plays a fundamental role in the regulation and alteration of the intranasal air flow characteristics.

The NVA is the site of maximum nasal resistance and acts as a diffuser where turbulence increases and velocity decreases. Concordantly, in all studies available the lowest flow velocity can be found directly behind the NVA resulting in a turbulent airflow with vortices. The airflow pattern is disrupted spreading the air over the entire mucosa of the adjoining turbinates with turbulences increasing and flow velocity decreasing.

When inhaled air passes the NVA, the laminar airflow changes into a turbulent one, prolonging and intensifying the contact of inhaled air to the surrounding mucosa.

Variations of the airflow pattern (turbulences, vortices, velocity of flow, volume flow, pressure conditions, distribution pattern and path lines) entail varying contact times of the inhaled air to the surrounding mucosa.

In laminar airflow, the direction is parallel to the mucosal surface, with only the air film closest to the surface touching the nasal mucosa (Figure 4). The increased kinetic energy of the turbulent airflow allows an intensified contact between inhaled air and mucosa.

The highest volume flows and flow velocities can be obtained in the centre of the nasal cavity followed by the inferior and middle meatus.
The highest air pressure is recorded at the head of the inferior and middle turbinate. The areas surrounding the turbinates show vortices of low velocity with turbulences. The turbinates mainly seem to be responsible for a close contact between air and nasal wall.
No significant differences in airflow characteristics between the right and left side of computational models of healthy noses could be observed (Figure 5).
During expiration the existing turbulent airflow predominating within the posterior and middle nasal segments is bundled and is transformed into a laminar one after passing the NVA (Figure 6).
In particular within the olfactory region a slow, turbulent airflow with static vortices is prevalent allowing an intensive contact between the inhaled air and the epithelium of the olfactory region. (Figure 5). Additionally, no relevant changes of airflow characteristics in the olfactory region due to alterations of respiratory volumes or during sniffing occur [104].
The flow velocity and flow volume within the paranasal sinuses is very low, reaching almost zero. Therefore, only very little exchange of air between nasal cavity and sinuses exists [108].

### 4.3.2 Simulation of intranasal temperature

The study group around Lindemann, Pless, Rettinger und Keck [111], [112], [113], [114], [115], [116] performed first-time CFD simulations of intranasal air temperature in combination with airflow pattern characteristics. The performed numerical simulations gained novel information and generated a visualisation of intranasal heating of the respiratory air. For the first time, the air temperature distribution within the entire nasal cavity combined with airflow patterns during respiration were illustrated in one computational model. In order to provide almost "physiological" conditions, values from recent in vivo measurements were applied as boundary conditions for the numerical simulation (respiratory volume, flow velocity, temperature of the wall and its distribution over the model, air temperature, wall conditions, etc.). In accordance to our in vivo temperature measurements on the nasal mucosa [44], [45], [48], the nasal wall temperature decreased from 34 °C (307 K) at the beginning to 30 °C (303 K) at the end of inspiration during the simulated respiratory cycles. In this case, the wall temperature of the nose model was chosen concordantly to the in vivo temperature measurements on the nasal mucosa.
The selected boundary conditions of the numerical simulations, however, are mere approximations to the physiological in vivo conditions. Therefore, the results of numerical simulations are generally depending on the set of the implemented boundary conditions. Numerical simulations always are approximations to "real" life.
Additionally, changes in intranasal air conditioning and airflow characteristics due to diverse nasal patho-morphologies like septal perforations, turbinate surgery and sinus surgery were simulated (see below) [114], [115], [116].
The major advantage of numerical simulations applying CFD is the 3-D display of air temperature distribution in any cutting plane within the entire nasal airways which cannot be provided by in vivo measurements due to their poor spatial resolution [111], [112], [113]. Furthermore, CFD is able to visualise the close relationship between airflow and intranasal heat transfer. Changes in air temperature during respiration are mainly caused by variations of airflow patterns (velocity, flow, vortices, path lines).
CFD also possess a high spatial and temporal resolution. The temperature distribution can be displayed in any cutting plane (coronal, axial, sagittal). In addition, the distribution of air temperature during in- and expiration as well as airflow path lines can be visualised in animated films (Figure 7, Figure 8). Under in vivo conditions, temperature changes of the nasal mucosa are the consequence of heat transfer between air and mucosa due to the existing temperature gradient. The existing temperature gradients between the mucosa (wall of the nose model) and the respiratory air leads to a heat exchange. The temperature distribution depends on the exact point of time during the respiratory cycle and the accurate intranasal detection site. There is a close relationship between the localised air temperature and airflow dynamics as changes in air temperature during respiration are mainly caused by variations of airflow patterns.
Distinct changes in air temperature during in- and expiration can be found in areas characterized by turbulent airflow with small vortices of low velocity, in particular around the inferior and middle turbinates.
The temperature results obtained by both in vivo measurements and numerical simulations highlight the important role of the anterior nasal segment including the NVA. This segment is the most effective part of the human nose when it comes to heating the incoming ambient air during inspiration and cooling of the exhaled air during expiration. This fact underlines once again the close relationship between airflow patterns and nasal air conditioning.
The simulated temperature distribution, absolute values of local temperatures and airflow patterns depend on the setting of boundary conditions (wall temperature, air temperature, inflow velocity, and so on) and realistic accuracy of the reconstructed nose model. Therefore, numerical simulations generally predict airflow dynamics and temperature distribution depending on the boundary conditions applied and always are **approximations**.
CFD simulations of intranasal humidification and filtration of particles are not yet published in the up-to-date literature, but are technically possible. The humidity exchange between the wall and air is difficult to simulate as the physiological processes of the humidity transfer can only be restrictively simulated. Additionally, active processes such as mucus secretion by mucosal glands and mucosal blood circulation cannot be adequately simulated.

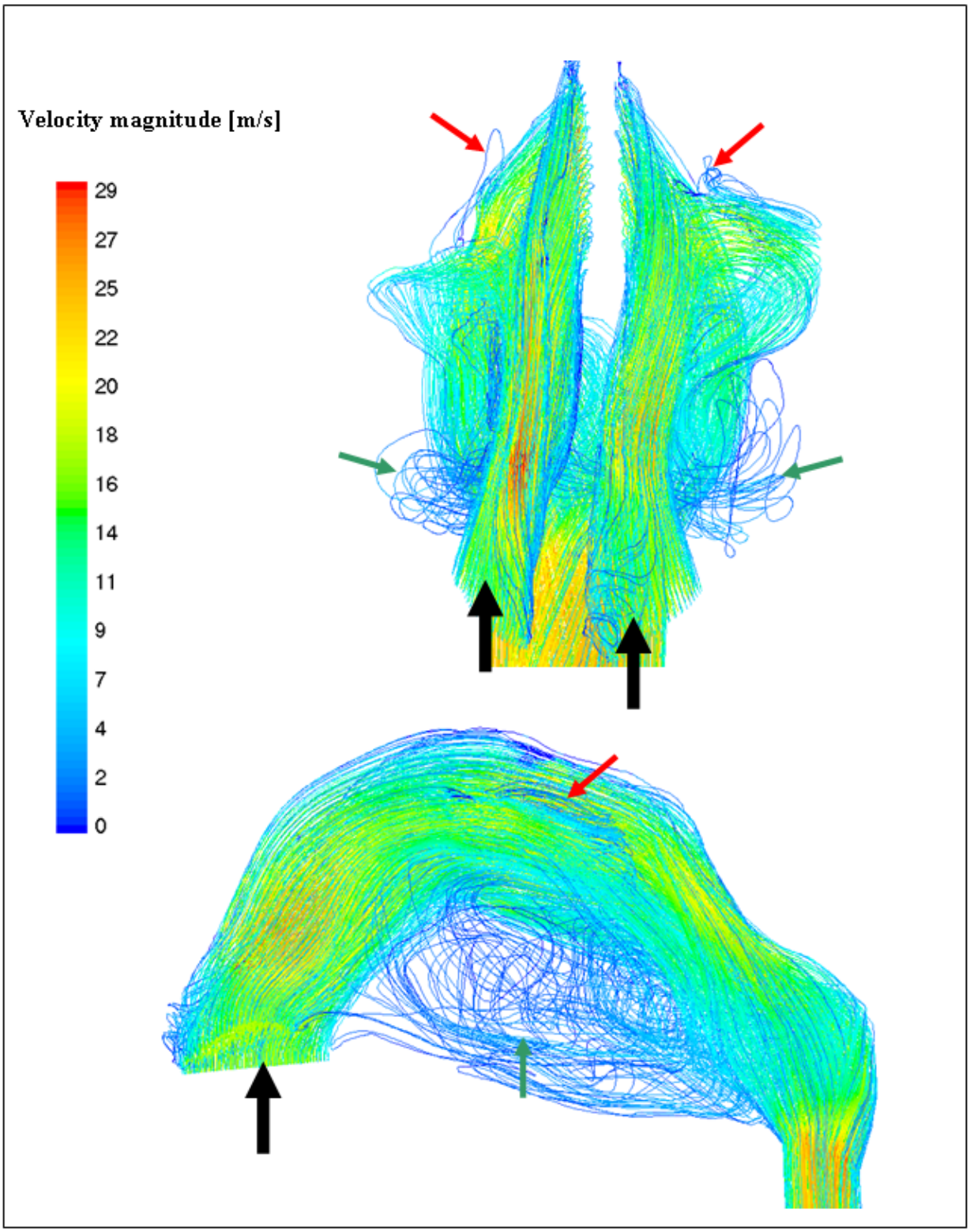


**Figure 5: Airflow patterns displayed by path lines coloured by velocity magnitude in anterior and lateral view within a computational model of a healthy nose during inspiration. The arrows mark regions of low velocity vortices within the area of the inferior (green arrows) and middle turbinate (red arrows).**

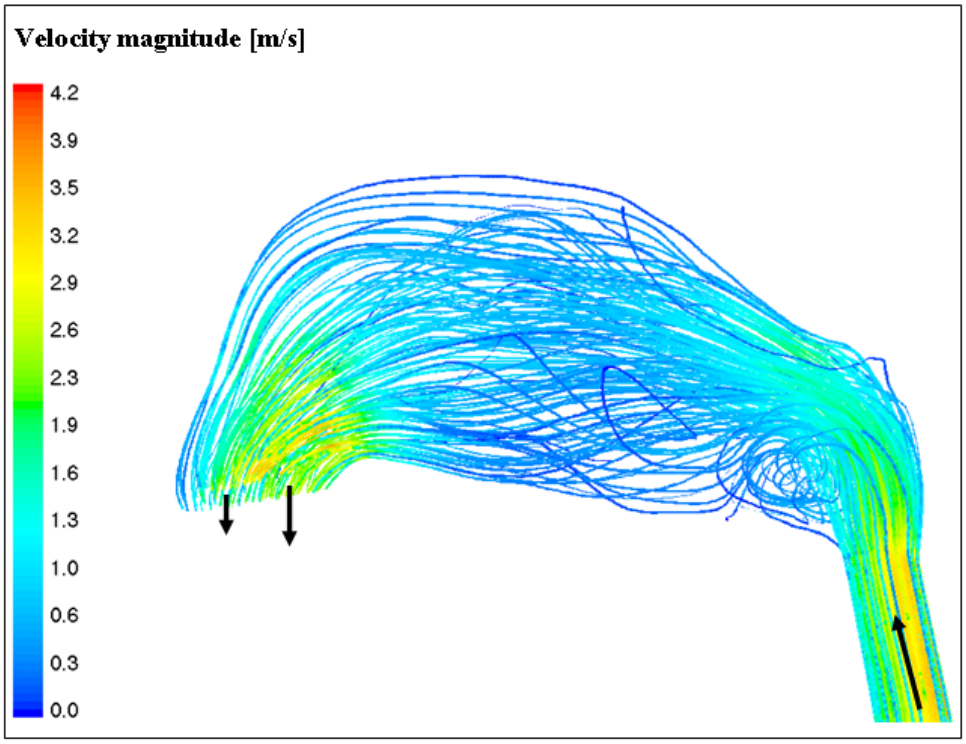


Figure 6: Airflow patterns displayed by path lines coloured by velocity magnitude within a computational model of a healthy nose during expiration.

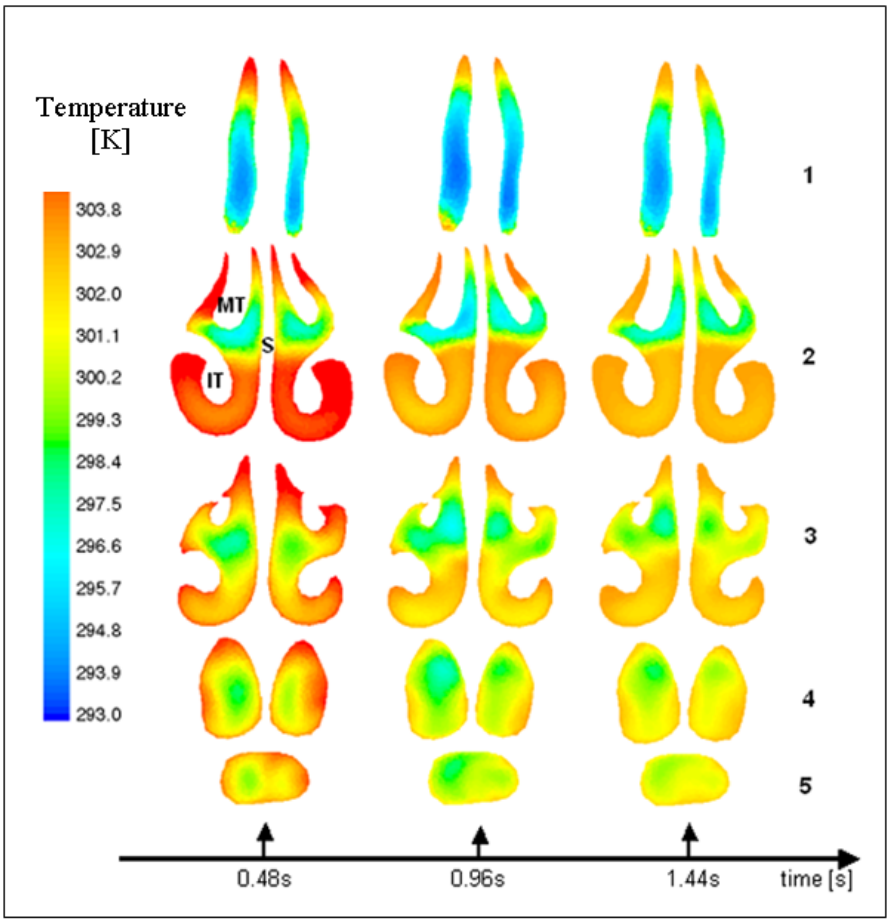


Figure 7: Inspiratory distribution of air temperature displayed on cutting planes at particular points of time within a computational model of a healthy nose. Nasal septum (S), inferior turbinate (IT) and middle turbinate (MT) are indicated.

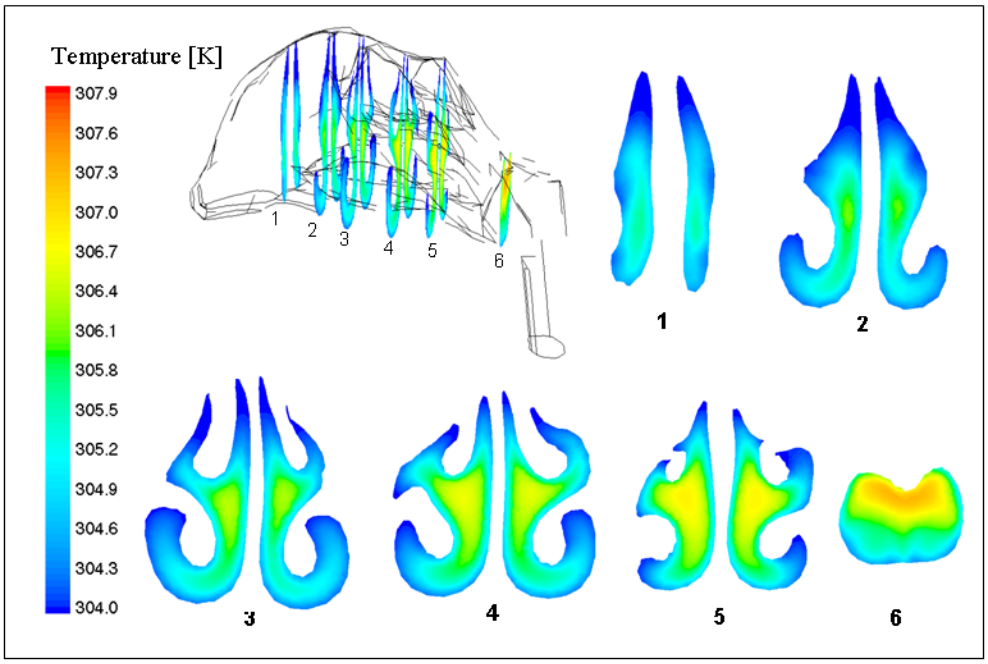


**Figure 8: Distribution of expiratory air temperature displayed on coronal cutting planes of the nasal cavities from anterior (1) to posterior (6) as demonstrated in the overview illustration within a computational model of a healthy nose.**

# 5 Intranasal air conditioning after nasal surgery

## 5.1 In vivo measurements in human

### 5.1.1 Turbinate surgery

Turbinate surgery is often combined with septoplasty, septorhinoplasty, or paranasal surgery. Therefore, it is generally difficult to analyze the effect of turbinate surgery itself on nasal air conditioning. Already in 1942 Moe investigated the effect of excessive turbinate surgery on the respiratory function in wide nasal cavities [130]. Moe found no significant deterioration of nasal climatisation due to turbinate resection compared to a healthy control group. However, a reduced increase in heat and moisture in surgically altered noses was obvious. Lindemann et al. [131] showed that nasal conditioning increased after septoplasty independent of simultaneous turbinoplasty. Therefore, anterior turbinoplasty with protection of the nasal mucosa seems to be a safe procedure without disturbance of nasal climatisation.

### 5.1.2 Septoplasty

Septoplasty has a clear benefit on the subjective nasal patency [132], [133]. Wiesmiller et al. showed in a recent study that septoplasty significantly improves nasal air-conditioning [134]. Four to six months after surgery intranasal warming and humidification of respiratory air increased.

### 5.1.3 Septorhinoplasty

In contrast to septoplasty, septorhinoplasty is characterized by surgical work on the bony pyramid and the cartilaginous framework of the nasal dorsum. Rozsasi et al. [135] showed a significant improvement of nasal conditioning in patients after septorhinoplasty. Widening of nasal airways was controlled by rhinomanometry.

### 5.1.4 Closure of septal perforations

Patients with nasal septal perforation suffer from nasal obstruction, crusting, nose bleeding, and whistling. Compared to healthy volunteers, patients presenting a septal perforation showed reduced nasal warming and moisturizing function during inspiration [136]. Surgical closure of septal perforations improved nasal air-conditioning [137].

### 5.1.5 Functional sinus surgery

One goal of functional sinus surgery is an improvement of sinus drainage and conservation of as much nasal mucosa as possible [138], [139]. In patients suffering from chronic rhinosinusitis without nasal polyps, sinus surgery does not affect nasal warming [140]. In patients with obstructing nasal polyps, heating and humidification of the nasal airways is significantly reduced compared to healthy noses. Already four to six weeks after endonasal sinus surgery, warming was significantly improved in patients with nasal polyposis, in contrast to humidification that was not altered after surgery [141]. Four to eight months after sinus surgery, humidity also increased [142].

### 5.1.6 Extensive sinus surgery

Radical, extensive sinus surgery and turbinate resection strongly decreases the ability of the nose to warm and humidify air. Drettner et al. investigated the climatisation function of the nose after partial maxillectomy. Compared to healthy controls, the operated noses showed significantly reduced temperature and humidity [49]. Nasal airways after radical turbinate resection, sinus surgery, and resection of the lateral nasal wall because of a unilateral inverted papilloma showed significantly reduced warming and humidification compared to nasal airways without surgery [143].

## 5.2 Numerical simulations

### 5.2.1 Simulation of turbinate surgery

Wexler et al. [107] investigated the effects of "conservative" turbinoplasty of the inferior turbinate on intranasal airflow characteristics in a CFD nose model. The simulated reduction of the inferior turbinate along its entire length led to a relevant reduction of pressure within the entire nasal cavity, even in non-adjacent regions of the turbinates. Additionally, an increased flow volume in the inferior and middle meatus had been described.
In a numerical study, Lindemann et al. [115] examined the effect of the complete unilateral resection of the inferior and middle turbinate on intranasal heating and airflow patterns. Due to the resection of the turbinates, the airflow pattern was seriously disturbed resulting in one large spacious vortex throughout the entire nasal cavity lacking any relevant flow towards the nasopharynx. As a consequence, a warm layer of air adjacent to the nasal wall prevented the effective blending and heating of the air within the centre of the air stream. Thus, relevant changes within the air temperature profile had mainly been found located adjacent to the nasal wall due to missing flow turbulences and the predominance of laminar airflow. Due to the elongated vortex within the nasal cavity, a reduced heating of the inspiratory air could be registered within the nasopharyngeal region on the modified side (Figure 9).

### 5.2.2 Simulation of septoplasty

Ozlugedik et al. [103] analysed the effect of a septoplasty on intranasal airflow patterns in a computational nose model. They clearly demonstrated that the numerical simulation of pathologically altered airflow patterns due to septal deviation is feasible. In addition, postoperative changes after a septoplasty can thus be approximated and predicted. Before virtual septoplasty the main airflow passed along the nasal floor with high flow velocity and largest pressure reductions over a short distance anterior to the septal deviation. After surgery, there was a significant decrease in flow velocity with a more even distribution of airflow within the entire nasal cavity including the inferior and middle meatus. The pressure reduction was most distinct in the area of the nasal valve region.

### 5.2.3 Simulation of septal perforations

The typical symptoms of patients with nasal septal perforations are crusting or nasal obstruction. The in vivo measured reduced heating and humidification of the inhaled air can be attributed to a pathologically altered airflow.
Numerical simulations on nose models with a nasal septum perforation showed that a disturbed airflow occurs in the area of the perforation [116], [118].
There is a spacious vortex including various localized vortices within the area of the septal perforation with turbulent flow lines. Streamlines hit against the posterior edge of the perforation. These findings strongly support the common clinical experience that crusting mainly occurs at the posterior edge of the perforation. Consequently, a disturbed intranasal temperature distribution results [116] (Figure 10). In addition, the temperature values are significantly reduced in the area of the perforation. These numerical results are very well comparable to fluid dynamics experiments [88].

### 5.2.4 Simulation of functional sinus surgery

Zhao et al. [106] demonstrated that functional sinus surgery with preoperative obstruction of the olfactory groove by nasal polyps leads to a normalisation of airflow and an increased volume flow in the area of the olfactory groove.
Xiong et al. [109] performed a flow analysis before and after a virtual functional sinus surgery in a computer model. This numerical simulation was able to demonstrate an increase in airflow especially in the area of the middle meatus, the maxillary-, ethmoid- and sphenoid sinus.

### 5.2.5 Simulation of extensive sinus surgery

In a numerical simulation in a nose and paranasal sinuses model, Lindemann et al. [114] investigated the consequences of radical sinus surgery on the intranasal airflow and heating of the respiratory air.
After unilateral resection of the turbinates, the lateral nasal wall and the anterior and posterior ethmoid cells of the right side, there were large static vortices throughout the entire nasal cavity, the maxillary sinus and the ethmoid sinus, lacking any relevant flow towards the nasopharynx. Within the static vortices a laminar flow is prevalent prohibiting an intense contact between air and surrounding nasal wall and therefore also preventing effective blending.
The airflow within the intact left nasal cavity remains straightforward towards the nasopharynx with only minor vortices. The areas around the turbinates show vortices of low velocity with turbulences. The turbinates mainly seem to be responsible for a close contact between air and nasal wall within the untouched left side.

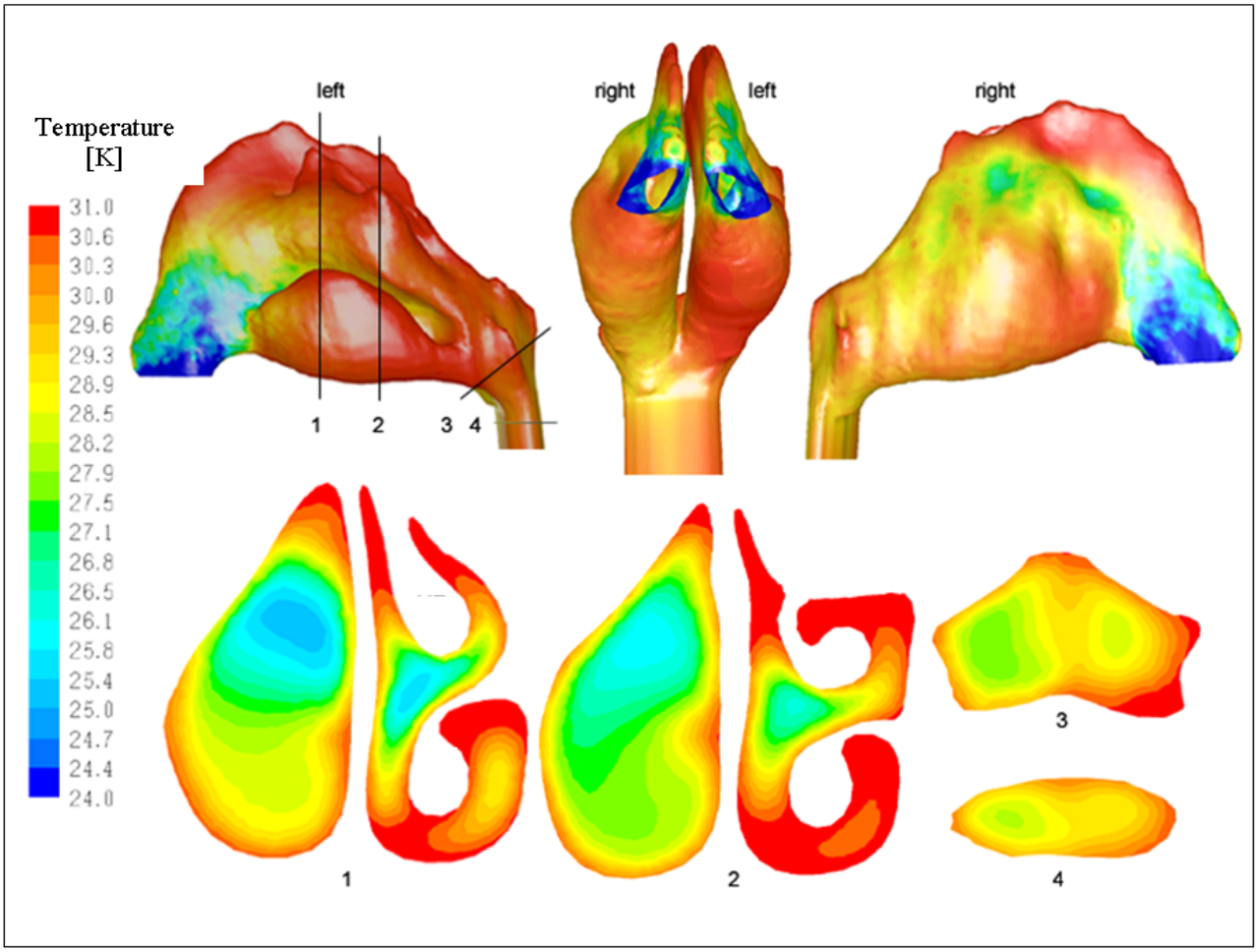


**Figure 9: Air temperature distribution within the right and the left nasal cavity displayed as surface plot (upper row) and on cutting planes (1–4) as indicated within a computational model of a nose with resection of the turbinates on the right side during inspiration.**

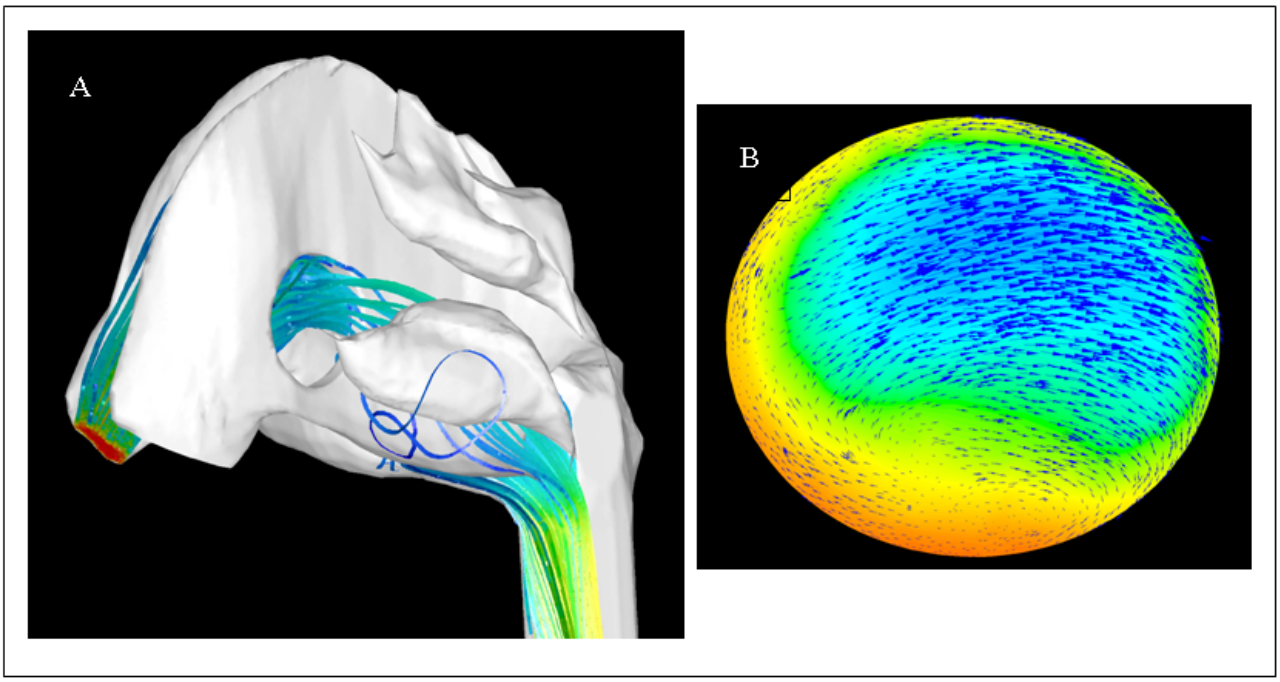


**Figure 10: Airflow patterns displayed by path lines within a computational model of a nose presenting a septal perforation during inspiration (within the complete model (A) and the area of the perforation (B)).**

A volume measurement of the nasal cavities provided a volume of 154 ml on the radically modified right nasal cavity and a volume of 68 ml on the unaffected left one. The surface area adds up to 201 $cm^2$ on the right side and 206 $cm^2$ on the left side. The ratio between nasal cavity volume and surface area is 0.8 on the right side and 0.3 on the left one.

The major reasons for the disturbed intranasal climatisation of the inspiratory air after radical sinus surgery seem to be a modified intranasal airflow, an enlarged nasal cavity volume, a reduction of the surface area in relation to the nasal cavity volume and the loss of the turbinates as a heating source.

Garcia et al. [110] simulated the effects of chronic atrophic rhinitis in a computational nose model with the nose geometry of a corresponding patient with a pathologically enlarged nasal cavity. They were also able to show abnormal airflow characteristics. There was a disturbed contact between air and surface of the model within the entire nasal cavity due to the low surface to volume ratio and the disturbed fluid dynamics.

# 6 For the future

The difficulties and technical restrictions of intranasal in vivo measurements depending on the detection site within the nose led to a wide variety of measurement approaches in the past in order to describe the climate within the nasal airways and the process of heat- and humidity exchange during inspiration and expiration.

With the described methods of numerical simulation applying computational fluid dynamics (CFD), now a more reliable and exact approach is given to gain deeper knowledge on the climatic processes occurring during the passage of the nasal airways, especially when it comes to planning rhinosurgical procedures.

The particular problems of anatomical variability between individuals, diverse mucosal swelling and other mucosal characteristics causing certain variations in airflow and intranasal climatisation are future tasks in the research field of numerical simulations.

Numerical simulations based on CT-scans of the nose and the paranasal sinuses before planned nasal surgery could be a helpful tool to approximate and predict a possible outcome of the operation and its effect on airflow and air conditioning. Numerical simulations could become part of the preoperative routine when planning rhinosurgery. It can not yet be anticipated and evaluated to its full extent if numerical simulations really lead to an improved outcome of rhinosurgical procedures.

# References


1. Calderón MA, Devalia JL, Davies RJ. Biology of nasal epithelium. In: Mygind N, Lildholdt T, eds. Nasal polyposis. An inflammatory disease and its treatment. Kopenhagen: Munksgaard; 1997. pp. 31-43.
2. Gwaltney JM, Jones JG, Kennedy DW. Medical management of sinusitis: educational goals and management guidelines. The International Conference on Sinus Disease. Ann Otol Rhinol Laryngol. 1995; Suppl: 16722-16730.
3. Ingelstedt S. Studies on the conditioning of air in the respiratory tract. Acta Otolaryngol. 1956; Suppl 131:1-80.
4. Heyder J, Armbruster L, Gebhart J, Grein E, Stahlhofen W. Total deposition of aerosol particles in the human respiratory tract for nose and mouth breathing. J Aerosol Sci. 1975; 6: 311-328. DOI: 10.1016/0021-8502(75)90020-8
5. Heyder J, Gebhart J, Rudolf G, Schiller CF, Stahlhofen W. Deposition of particles in the human respiratory tract in the size range 0.005-15 µm. J Aerosol Sci. 1986; 17: 811-825. DOI: 10.1016/0021-8502(86)90035-2
6. Deitmer T. Moderne Funktionsdiagnostik der Nase und der Nasennebenhöhlen. Eur Arch Otorhinolaryngol. 1996; Suppl I:1-71.
7. Keck T, Leiacker R, Schick M, Rettinger G, Kühnemann S. Temperatur- und Feuchteprofil der Nase vor und nach Schleimhautabschwellung durch Xylometazolin. Laryngorhinootologie. 2000; 79: 749-752. DOI: 10.1055/s-2000-9138
8. Stuart BO. Deposition and clearance of inhaled particles. Environ Health Persp. 1984; 55: 369-390. DOI: 10.2307/3429715
9. Cole P. Recordings of respiratory air temperature. J Laryngol Otol. 1954; 68: 295-307. DOI: 10.1017/S0022215100049690
10. Cole P. Respiratory mucosal vascular responses, air conditioning and thermoregulation. J Laryngol Otol. 1954; 68: 613-622. DOI: 10.1017/S0022215100050040
11. Ingelstedt S. Studies on the conditioning of air in the respiratory tract. Acta Otolaryngol. 1956; Suppl 131: 1-80.
12. Ingelstedt S, Ivstam B. Study on the humidifying capacity of the nose. Acta Otolaryngol. 1951; 49: 286-290. DOI: 10.3109/00016485109119255
13. Rouadi P, Baroody FM, Abbott D, Naureckas E, Solway J, Nacleiro RM. A technique to measure the ability of the human nose to warm and humidify air. J Appl Physiol. 1999; 87:400-406.
14. Cheng YS, Hansen GK, Su YF, Yeh HC, Morgan KT. Deposition of ultrafine aerosols in rat nasal molds. Toxicol Appl Pharmacol. 1990; 106: 222-233. DOI: 10.1016/0041-008X(90)90242-M
15. Cheng YS, Yeh HC, Swift DL. Aerosol deposition in human nasal airway for particles 1 nm to 20 µm: a model study. Radiat Prot Dosimetry. 1991; 38: 41-47.
16. Mollier R. Das ix-Diagramm für Dampfluftgemische. Z Ver Dt Ing. 1929; 73:1009-1013.
17. Weber D. Das Mollier-Diagramm. In: Weber D, Hrsg. Technische Feuchtemessung. Essen: Vulkan Verlag; 1995. pp. 26-37.
18. Kern EB. Surgical approaches to abnormalities of the nasal valve. Rhinology. 1978; 16: 165-189.
19. Bruintjes TD, van Olphen AF, Hillen B, Huizing EH. A functional anatomic study of the relationship of the nasal cartilages and muscles to the nasal valve area. Laryngoscope. 1998; 108: 1025-1032. DOI: 10.1097/00005537-199807000-00014
20. Shaida AM, Kenyon GS. The nasal valves: changes in anatomy and physiology in normal subjects. Rhinology. 2000; 38: 7-12.
21. Widdicombe J. Microvascular anatomy of the nose. Allergy. 1997; 52 Suppl 40: 7-11. DOI: 10.1111/j.1398-9995.1997.tb04877.x
22. Lang J. Nasal cavity. In: Lang J, ed. Clinical anatomy of the nose, nasal cavity and paranasal sinuses. New York: Thieme Medical Publishers; 1989. pp. 31-55.

23. Swift DL, Proctor DF. Access of air to the respiratory tract. In: Brain JD, Proctor DF, Reid LM, eds. Respiratory defence mechanisms. New York: Marcel Dekker, Inc; 1977. pp. 63-93.

24. Mygind N, Pedersen M, Nielsen MH. Morphology of the upper airway epithelium. In: Proctor DF, Andersen IB, eds. The nose. Upper airway physiology and the atmospheric environment. Amsterdam, New York, Oxford: Elsevier Biomedical Press; 1982. pp. 71-97.

25. Kaliner MA, Shelhamer JH, Borson DB, Patow CA, Marom Z, Nadel JA. Respiratory mucus. In: Kaliner MA, Barnes PJ, eds. The airways. Neural control in health and disease. New York, Basel: Marcel Dekker, Inc; 1988. pp. 575-593.

26. Proctor DF. The mucociliary system. In: Proctor DF, Andersen IB, eds. The nose. Upper airway physiology and the atmospheric environment. Amsterdam, New York, Oxford: Elsevier Biomedical Press; 1982. pp. 245-278.

27. Basbaum CB. Regulation of airway secretory cells. Clin Chest Med. 1986; 7: 231-237.

28. Cole P. Modification of inspired air. In: Proctor DF, Andersen IB, eds. The nose. Upper airway physiology and the atmospheric environment. Amsterdam, New York, Oxford: Elsevier Biomedical Press; 1982. pp. 351-375.

29. Cauna N, Cauna D, Hinderer KH. Innervation of human nasal glands. J Neurocytol. 1972; 1: 49-60. DOI: 10.1007/BF01098645

30. Cauna N. Blood and nerve supply of the nasal lining. In: Proctor DF, Andersen IB, eds. The nose. Upper airway physiology and the atmospheric environment. Amsterdam, New York, Oxford: Elsevier Biomedical Press BV; 1982. pp. 45-69.

31. Dahlström A, Fuxe K. The adrenergic innervation of the nasal mucosa of certain mammals. Acta Otolaryngol. 1965; 59: 65-72. DOI: 10.3109/00016486509128547

32. Olsson P, Bende M, Ohlin P. The Laser Doppler Flowmeter for measuring microcirculation in human nasal mucosa. Acta Otolaryngol. 1985; 99: 133-139. DOI: 10.3109/00016488509119155

33. Lund VJ. Nasal physiology: Neurochemical receptors, nasal cycle, and ciliary action. Allergy Asthma Proc. 1996; 17: 179-84. DOI: 10.2500/108854196778996877

34. Cole P. Respiratory mucosal vascular responses, air conditioning and thermoregulation. J Laryngol Otol. 1954; 68: 613-622. DOI: 10.1017/S0022215100050040

35. Walker JEC, Wells RE, Merrill EW. Heat and water exchange in the respiratory tract. Am J Med. 1961; 30: 259-267. DOI: 10.1016/0002-9343(61)90097-3

36. Willatt DJ. Continuous infrared thermometry of the nasal mucosa. Rhinology. 1993; 31: 63-67.

37. Cole P. Nasal and oral airflow resistors. Site, function, and assessment. Arch Otolaryngol Head Neck Surg. 1992; 118: 790-793.

38. Mlynski G. Strömung und Konditionierung der Atemluft. Laryngorhinootologie. 2000; 79: 636-638. DOI: 10.1055/s-2000-8287

39. Elad D, Liebenthal R, Wenig BL, Einav S. Analysis of air flow patterns in the human nose. Med Biol Eng Comput. 1993; 31: 585-592. DOI: 10.1007/BF02441806

40. Kelly JT, Prasad AK, Wexler AS. Detailed flow patterns in the nasal cavity. J Appl Physiol. 2000; 89: 323-337.

41. Webb P. Air temperatures in respiratory tracts of resting subjects in cold. J Appl Physiol. 1951; 4: 378-382.

42. Keck T, Leiacker, Heinrich A, Kühnemann S, Rettinger G. Humidity and temperature profile in the nasal cavity. Rhinology. 2000; 38: 167-171.

43. Keck T, Leiacker R, Riechelmann H, Rettinger G. Temperature profile in the nasal cavity. Laryngoscope. 2000; 110: 651-654. DOI: 10.1097/00005537-200004000-00021

44. Cole P. Further observations on the conditioning of respiratory air. J Laryngol Otol. 1953;67:669-681. DOI: 10.1017/S0022215100049161

45. McFadden ER Jr, Pichurko BM, Bowman HF, Ingenito E, Burns S, Dowling N, Solway J. Thermal mapping of the airways in humans. J Appl Physiol. 1985; 58: 564-570.

46. Lindemann J, Wiesmiller K, Kastl KG. Dynamic nasal infrared thermography in patients with nasal septal perforations. Am J Rhinol. 2009; 23: 471-4. DOI: 10.2500/ajra.2009.23.3351

47. Kastl KG, Wiesmiller KM, Lindemann J. Dynamic infrared thermography of the nasal vestibules: a new method. Rhinology. 2009;47:89-92.

48. Liese W, Joshi R, Cumming G. Humidification of respired gas by nasal mucosa. Ann Otol. 1973; 82: 330-332.

49. Drettner B, Falck B, Simon H. Measurements of the air conditioning capacity of the nose during normal and pathological conditions and pharmacological influence. Acta Otolaryngol. 1977; 84: 266-277. DOI: 10.3109/00016487709123966

50. Drettner B, Kumlien J. Experimental studies of the human nasal air conditioning capacity. Acta Otolaryngol. 1981; 91: 605-609. DOI: 10.3109/00016488109138547

51. Perwitzschky R. Die Temperatur- und Feuchtigkeitsverhältnisse der Atemluft in den Luftwegen. I. Mitteilung. Arch f Hals-, Nasen- u Ohrenheilk. 1928; 117: 1-36.

52. Perwitzschky R. Die Temperatur- und Feuchtigkeitsverhältnisse der Atemluft in den Luftwegen. II. Mitteilung. Arch f Hals-, Nasen- u Ohrenheilk. 1930; 125: 1-22.

53. Seeley LE. Study of changes in the temperature and water vapor content of respired air in the nasal cavity. Heating Piping and Air Conditioning. 1940; 12: 377-388.

54. Primiano FP, Montague FW, Saidel GM. Measurement system for respiratory water vapor and temperature dynamics. J Appl Physiol Respirat Environ Exercise Physiol. 1984; 56: 1679-1685.

55. Primiano FP, Saidel GM, Montague FW, Kruse KL, Green CG, Horowitz JG . Water vapour and temperature dynamics in the upper airways of normal and CF subjects. Eur Respir J. 1988; 1: 407-414.

56. Dick W. Aspects of humidification: requirements and techniques. Int Anesthesiol Clin. 1974; 12: 217-239. DOI: 10.1097/00004311-197412040-00013

57. Kohler P, Rimek A, Albrecht M, Frankenberger H, Mertins W, van Ackern K. Sind Feuchtigkeitsfilter in der Inspirationsluft während Narkosebeatmung notwendig? Neue In-vivo-Methode zur Feuchtigkeitsmessung im Atemgas. Anästhesiol Intensivmed Notfallmed Schmerzther. 1992; 27: 149-155. DOI: 10.1055/s-2007-1000270

58. Wissing H, Kuhn I, Kessler P. Das Wärme-Feuchte-Profil des PhysioFlex. Untersuchungen am Modell. Anaesthesist. 1997; 46: 201-206. DOI: 10.1007/s001010050392

59. Kaufman JW, Farahmand K. In vivo measurements of human oral cavity heat and water vapor transport. Respiratory Physiology and Neurobiology. 2006; 150: 260-277. DOI: 10.1016/j.resp.2005.05.016

60. Akerlund A, Bende M. Nasal mucosal temperature and the effect of acute infective rhinitis. Clin Otolaryngol. 1989; 14: 529-534. DOI: 10.1111/j.1365-2273.1989.tb00418.x

61. Hair GE, Fischer ND, Preslar MJ. Humidification of air by nasal mucosa. A method of study. Laryngoscope. 1969; 79: 375-381. DOI: 10.1288/00005537-196903000-00005

62. Nowak E. Moisture measurement with capacitive polymer humidity sensors. Sensors. 1996; 13: 86-91.

63. Ohhashi T, Sakaguchi M, Tsuda T. Human perspiration measurement. Physiol Meas. 1998; 19: 449-461. DOI: 10.1088/0967-3334/19/4/001

64. Wilson AC, Barnes TH, Seakins PJ, Rolfe TG, Meyer EJ. A low-cost, high-speed, near-infrared hygrometer. Rev Sci Instrum. 1995; 66: 5618-5624. DOI: 10.1063/1.1146028

65. Kumlien J. Persönliche Mitteilung. 2000.

66. Ophir D, Elad Y, Fishler E, Fink A, Marshak G. Effects of elevated intranasal temperature on subjective and objective findings in perennial rhinitis. Ann Otol Rhinol Laryngol. 1988; 97: 259-263.

67. Assanasen P, Baroody FM, Naureckas E, Naclerio RM. Warming of feet elevates nasal mucosal surface temperature and reduces the early response to nasal challenge with allergen. J Allergy Clin Immunol. 1999; 104: 285-293. DOI: 10.1016/S0091-6749(99)70368-4

68. Cole P. Air conditioning. In: Cole P, ed. The respiratory role of the upper airways. St. Louis: Mosby Year Book; 1992. pp. 102-106.

69. Keck T, Leiacker R, Meixner D, Kühnemann S, Rettinger G. Erwärmung der Atemluft in der Nase. HNO. 2001; 49: 36-40. DOI: 10.1007/s001060050705

70. Heywang F, Nücke E, Timm J, Timm W. Wärmelehre. In: Heywang F, Nücke E, Timm J, Timm W, Hrsg. Physik für Techniker. Hamburg: Verlag Handwerk und Technik; 1996. pp. 155-203.

71. Mercke U. The influence of temperature on mucociliary activity: temperature range 40°C-50°C. Acta Otolaryngol. 1974; 78: 253-258. DOI: 10.3109/00016487409126352

72. Mercke U, Hakansson CH, Toremalm NG. The influence of temperature on mucociliary activity: temperature range 20°C-40°C. Acta Otolaryngol. 1974; 78: 444-450. DOI: 10.3109/00016487409126378

73. Swift DL, Proctor DF. Access of air to the respiratory tract. In: Brain JD, Proctor DF, Reid LM, eds. Respiratory defence mechanisms. New York: Marcel Dekker, Inc; 1977. pp. 63-93.

74. Keck T, Leiacker R, Lindemann J, Rettinger G, Kühnemann S. Endonasales Temperatur- und Feuchteprofil nach Exposition zu verschieden klimatisierter Einatemluft. HNO. 2001; 49: 372-377. DOI: 10.1007/s001060050765

75. Olsson P, Bende M. Influence of environmental temperature on human nasal mucosa. Ann Otol Rhinol Laryngol. 1985; 94: 153-155.

76. Fontanari P, Burnet H, Zattara-Hartmann MC, Jammes Y. Changes in airway resistance induced by nasal inhalation of cold dry, dry, or moist air in normal individuals. J Appl Physiol. 1996; 81: 1739-1743.

77. Jankowski R, Philip G, Togias A, Naclerio R. Demonstration of bilateral cholinergic secretory response after unilateral nasal cold, dry air challenge. Rhinology. 1993; 31: 97-100.

78. Philip G, Jankowski R, Baroody FM, Naclerio RM, Togias AG. Reflex activation of nasal secretion by unilateral inhalation of cold dry air. Am Rev Respir Dis. 1993; 148: 1616-1622.

79. Rozsasi A, Leiacker R, Keck T. Nasal conditioning in perennial allergic rhinitis after nasal allergen challenge. Clin Exp Allergy. 2004; 34: 1099-104. DOI: 10.1111/j.1365-2222.2004.01996.x

80. Fabricant ND. The topical temperature of clinically normal nasal and pharyngeal mucous membranes. Arch Otolaryngol. 1957; 66: 275-277.

81. Jun Y, Qingping Z. Twenty-three cases of atrophic rhinitis treated by deep puncture at three points in the nasal region. J Trad Chin Med. 1999; 19: 115-117.

82. Lindemann J, Leiacker R, Rettinger G, Keck T. Nasal mucosal temperature during respiration. Clin Otolaryngol. 2002; 27: 135-139. DOI: 10.1046/j.1365-2273.2002.00544.x

83. Lindemann J, Leiacker R, Rettinger G, Keck T. The effect of topical xylometazoline on the mucosal temperature of the nasal septum. Am J Rhinol. 2002; 16: 229-234.

84. Lindemann J, Leiacker R, Wiesmiller K, Rettinger G, Keck T. Immediate effect of benzalkonium-chloride in decongestant nasal spray on the human nasal mucosal temperature. Clin Otolaryngol. 2004; 29: 357-361. DOI: 10.1111/j.1365-2273.2004.00837.x

85. Molony N, Blackwell C, Busuttil A. The effect of prone posture on nasal temperature in children in relation to induction of staphylococcal toxins implicated in sudden infant death syndrome. FEMS Immunol. Med. Microbiol. 1999; 25: 103-108. DOI: 10.1111/j.1574-695X.1999.tb01333.x

86. Willatt DJ. Continuous infrared thermometry of the nasal mucosa. Rhinology. 1993; 31: 63-67.

87. Lindemann J, Sannwald D, Wiesmiller K. Age-related changes in intranasal air conditioning in the elderly. Laryngoscope. 2008; 118: 1472-5. DOI: 10.1097/MLG.0b013e3181758174

88. Grutzenmacher S, Lang C, Saadi R, Mlynski G. First findings about the nasal airflow in noses with septal perforation. Laryngorhinootologie. 2002; 81: 276-279.

89. Hahn I, Scherer PW, Mozell MM. Velocity profiles measured for airflow through a large-scale model of the human nasal cavity. J Appl Physiol. 1993; 75: 2273-2287.

90. Hess MM, Lamprecht J, Horlitz S. Experimentelle Untersuchungen in der Nasenhaupthöhle des Menschen im Nasenmodell. Laryngo Rhino Otol. 1992; 71: 467. DOI: 10.1055/s-2007-997334

91. Hornung DE, Leopold DA, Youngentob SL, Sheehe PR, Gagne GM, Thomas FD, Mozell M. Airflow pattern in a human nasal model. Arch Otolaryngol Head Neck Surg. 1987; 113: 169-172.

92. Levine SC, Levine H, Jacobs G, Kasick J. A technique to model the nasal airway for aerodynamic study. Arch Otolaryngol Head Neck Surg. 1986; 4: 442-449.

93. Masing H. Experimentelle Untersuchungen über die Strömung im Nasenmodell. Arch Klin Exp Ohren Nasen Kehlkopfheilkd. 1967; 189: 59-70. DOI: 10.1007/BF00417416

94. Mink JP. Physiologie der oberen Luftwege. Leipzig: Verlag FCW Vogel; 1920.

95. Mlynski G, Grutzenmacher S, Plontke S, Mlynski B, Lang C. Correlation of nasal morphology and respiratory function. Rhinology. 2001; 39: 197-201.

96. Proctor DF. Airborne disease and the upper respiratory tract. Bacteriol Rev. 1966; 30: 498-513.

97. Proctor DF, Swift DL. Temperature and water vapor adjustment. In: Respiratory Defense Mechanisms, Part I. New York: Dekker M Inc; 1977. pp. 95-124.

98. Proetz AW. Air currents in the upper respiratory tract and their clinical importance. Ann Otol Rhinol Laryngol. 1951; 60: 439-467.

99. Scherer PW, Hahn II, Mozell MM. The biophysics of nasal airflow. Otolaryngol Clin North Am. 1989; 22: 265-278.

100. Simmen D, Scherrer JL, Moe K, Heinz B. A dynamic and direct visualization model for the study of nasal airflow. Arch Otolaryngol Head Neck Surg. 1999; 125: 1015-1021.

101. Tonndorf J. Der Weg der Atemluft durch die menschliche Nase. Arch Ohr-, Nase-, Kehlk Heilk. 1939; 146: 41. DOI: 10.1007/BF01583671

102. Uddstromer M. Nasal respiration. Acta Oto Laryngologica. 1940; Suppl 42.

103. Ozlugedik S, Nakiboglu G, Sert C, Elhan A, Tonuk E, Akyar S, Tekdemir I. Numerical study of the aerodynamic effects of septoplasty and partial lateral turbinectomy. Laryngoscope. 2008; 118: 330-334. DOI: 10.1097/MLG.0b013e318159aa26

104. Ishikawa S. Nakayama T. Watanabe M. Matsuzawa T. Flow mechanisms in the human olfactory groove: numerical simulation of nasal physiological respiration during inspiration, expiration, and sniffing. Arch Otolaryngol Head Neck Surg. 2009; 135: 156-162. DOI: 10.1001/archoto.2008.530

105. Wen J. Inthavong K. Tu J. Wang S. Numerical simulations for detailed airflow dynamics in a human nasal cavity. Resp Physiol Neurobiol. 2008; 161: 125-135. DOI: 10.1016/j.resp.2008.01.012

106. Zhao K. Pribitkin EA. Cowart BJ. Rosen D. Scherer PW. Dalton P. Numerical modeling of nasal obstruction and endoscopic surgical intervention: outcome to airflow and olfaction. Am J Rhinol. 2006; 20: 308-316. DOI: 10.2500/ajr.2006.20.2848

107. Wexler D. Segal R. Kimbell J. Aerodynamic effects of inferior turbinate reduction: computational fluid dynamics simulation. Arch Otolaryngol Head Neck Surg. 2005;131(12):1102-7. DOI: 10.1001/archotol.131.12.1102

108. Xiong GX. Zhan JM. Jiang HY. Li JF. Rong LW. Xu G. Computational fluid dynamics simulation of airflow in the normal nasal cavity and paranasal sinuses. Am J Rhinol. 2008; 22: 477-482. DOI: 10.2500/ajr.2008.22.3211

109. Xiong G, Zhan J, Zuo K, Li J, Rong L, Xu G. Numerical flow simulation in the post-endoscopic sinus surgery nasal cavity. Med Biol Eng Comput. 2008; 46: 1161-1167. DOI: 10.1007/s11517-008-0384-1

110. Garcia GJ. Bailie N. Martins DA. Kimbell JS. Atrophic rhinitis: a CFD study of air conditioning in the nasal cavity. J Appl Physiol. 2007; 103: 1082-1092. DOI: 10.1152/japplphysiol.01118.2006

111. Lindemann J, Keck T, Wiesmiller K, Sander B, Brambs HJ, Rettinger G, Pless D. A numerical simulation of intranasal air temperature during inspiration. Laryngoscope. 2004; 114: 1037-1041. DOI: 10.1097/00005537-200406000-00015

112. Pless D, Keck T, Wiesmiller K, Rettinger G, Aschoff AJ, Fleiter TR, Lindemann J. Numerical simulation of air temperature and airflow patterns in the human nose during expiration. Clin Otolaryngol. 2004; 29: 642 -647. DOI: 10.1111/j.1365-2273.2004.00862.x

113. Lindemann J, Keck T, Wiesmiller KM, Sander B, Brambs HJ, Rettinger G, Pless D. Nasal air temperature and airflow during respiration in numerical simulation based on multislice computed tomography scan. Am J Rhinol Rhinol. 2006; 20: 219-223.

114. Lindemann J, Brambs HJ, Keck T, Wiesmiller KM, Rettinger G, Pless D. Numerical simulation of intranasal air flow after radical sinus surgery. Am J Otolaryngol. 2005; 26: 175-180. DOI: 10.1016/j.amjoto.2005.02.010

115. Lindemann J, Keck T, Wiesmiller KM, Rettinger G, Brambs HJ, Pless D. Numerical simulation of intranasal air flow and temperature after resection of the turbinates. Rhinology. 2005; 43: 24-28.

116. Pless D, Keck T, Wiesmiller KM, Lamche R, Aschoff AJ, Lindemann J. Numerical simulation of airflow patterns and air temperature distribution during inspiration in a nose model with septal perforation. Am J Rhinol. 2004; 18: 357-362.

117. Bockholt U, Mlynski G, Muller W, Voss G. Rhinosurgical therapy planning via endonasal airflow simulation. Comput Aided Surg. 2000; 5: 175-179. DOI: 10.1002/1097-0150(2000)5:3<175::AID-IGS5>3.0.CO;2-1

118. Grant O, Bailie N, Watterson J, Cole J, Gallagher G, Hanna B. Numerical model of a nasal septal perforation. Medinfo. 2004; 11: 1352-1356.

119. Keyhani K, Scherer PW, Mozell MM. Numerical simulation of airflow in the human nasal cavity. J Biomech Eng. 1995; 117: 429-441. DOI: 10.1115/1.2794204

120. Muller-Wittig W, Mlynski G, Weinhold I, Bockholt U, Voss G. Nasal airflow diagnosis--comparison of experimental studies and computer simulations. Stud Health Technol Inform. 2002; 85: 311-317.

121. Tarabichi M, Fanous N. Finite element analysis of airflow in the nasal valve. Arch Otolaryngol Head Neck Surg. 1993; 119: 638-642.

122. Weinhold I, Mlynski G. Numerical simulation of airflow in the human nose. Eur Arch Otorhinolaryngol. 2004; 261: 452-455. DOI: 10.1007/s00405-003-0675-y

123. Zhao K, Scherer PW, Hajiloo SA, Dalton P. Effect of anatomy on human nasal air flow and odorant transport patterns: implications for olfaction. Chem Senses. 2004; 29: 365-379. DOI: 10.1093/chemse/bjh033

124. Martonen TB, Quan L, Zhang Z, Musante CJ. Flow simulation in the human upper respiratory tract. Cell Biochem Biophys. 2002; 37: 27-36. DOI: 10.1385/CBB:37:1:27

125. Martonen TB, Zhang Z, Yu G, Musante CJ. Three-dimensional computer modeling of the human upper respiratory tract. Cell Biochem Biophys. 2001; 35: 255-261. DOI: 10.1385/CBB:35:3:255

126. Balashazy I, Farkas A, Szoke I, Hofmann W, Sturm R. Simulation of deposition and clearance of inhaled particles in central human airways. Radiat Prot Dosimetry. 2003; 105: 129-132.

127. Calay RK, Kurujareon J, Holdo AE. Numerical simulation of respiratory flow patterns within human lung. Respir Physiolo Neurobiol. 2002; 130: 201-221. DOI: 10.1016/S0034-5687(01)00337-1

128. Hegedus CJ, Balashazy I, Farkas A. Detailed mathematical description of the geometry of airway bifurcations. Respir Physiol Neurobiol. 2004; 141: 99-114. DOI: 10.1016/j.resp.2004.03.004

129. Nowak N, Kakade PP, Annapragada AV. Computational fluid dynamics simulation of airflow and aerosol deposition in human lungs. Ann Biomed Eng. 2003; 31: 374-390. DOI: 10.1114/1.1560632

130. Moe R. The effect on the respiratory functions of the nose of the lumen-dilating nasal operations. Acta Otolaryngol. 1942; Suppl 45: 5-146.

131. Lindemann J, Keck T, Leiacker R, Dzida R, Wiesmiller K. Early influence of bilateral turbinoplasty combined with septoplasty on intranasal air conditioning. Am J Rhinol. 2008; 22:542-545. DOI: 10.2500/ajr.2008.22.3224

132. Arunachalam PS, Kitcher E, Gray J, Wilson JA. Nasal septal surgery: evaluation of symptomatic and general health outcomes. Clin Otolaryngol Allied Sci. 2001; 26: 367-370. DOI: 10.1046/j.0307-7772.2001.00481.x

133. Stewart MG, Smith TL, Weaver EM. Outcomes after nasal septoplasty: results from the Nasal Obstruction Septoplasty Effectiveness (NOSE) study. Otolaryngol Head Neck Surg. 2004; 130: 283-290. DOI: 10.1016/j.otohns.2003.12.004

134. Wiesmiller K, Keck T, Rettinger G, Leiacker R, Dzida R, Lindemann J. Nasal air conditioning in patients before and after septoplasty with bilateral turbinoplasty. Laryngoscope. 2006; 116: 890-894. DOI: 10.1097/01.mlg.0000201995.02171.ea

135. Rozsasi A, Leiacker R, Kühnemann S, Lindemann J, Kappe T, Rettinger G, Keck T. The impact of septorhinoplasty and anterior turbinoplasty on nasal conditioning. Am J Rhinol. 2007; 21: 302-306. DOI: 10.2500/ajr.2007.21.3036

136. Lindemann J, Kuhnemann S, Stehmer V, Leiacker R, Rettinger G, Keck T. Temperature and humidity profile of the anterior nasal airways of patients with nasal septal perforation. Rhinology. 2001; 39: 202-206.

137. Lindemann J, Leiacker R, Stehmer V, Rettinger G, Keck T. Intranasal temperature and humidity profile in patients with nasal septal perforation before and after surgical closure. Clin Otolaryngol Allied Sci. 2001; 26:433-437. DOI: 10.1046/j.1365-2273.2001.00501.x

138. Stammberger H, Posawetz W. Functional endoscopic sinus surgery. Concept, indications and results of the Messerklinger technique. Eur Arch Otorhinolaryngol. 1990; 247: 63-76.

139. Kennedy DW, Senior BA. Endoscopic sinus surgery: A review. Prim Care. 1998; 25: 703-720.

140. Keck T, Leiacker R, Kuhnemann S, Rettinger G. Heating of air in the nasal airways in patients with chronic sinus disease before and after sinus surgery. Clin Otolaryngol Allied Sci. 2001; 26: 53-58. DOI: 10.1046/j.1365-2273.2001.00429.x

141. Papp J, Leiacker R, Keck T, Rozsasi A, Kappe T. Nasal air-conditioning in patients with chronic rhinosinusitis and nasal polyposis. Arch Otolaryngol Head Neck Surg. 2008; 134: 931-935. DOI: 10.1001/archotol.134.9.931

142. Kappe T, Papp J, Rozsasi A, Leiacker R, Rettinger G, Keck T. Nasal conditioning after endonasal surgery in chronic rhinosinusitis with nasal polyps. Am J Rhinol. 2008; 22: 89-94. DOI: 10.2500/ajr.2008.22.3128

143. Lindemann J, Leiacker R, Sikora T, Rettinger G, Keck T. Impact of unilateral sinus surgery with resection of the turbinates by means of midfacial degloving on nasal air conditioning. Laryngoscope. 2002; 112: 2062-2066. DOI: 10.1097/00005537-200211000-00029

**Corresponding authors:**

Prof. Dr. Tilman Keck
Department of Otorhinolaryngology, Head, Neck, and Facial Plastic Surgery, Elisabethinen-Hospital GmbH, Academic hospital of the University of Graz, Elisabethinergasse 14, 8020 Graz, Austria, Tel: +43-316-7063-1140, Fax: +43-316-7063-1620
kecktill@aol.com

Prof. Dr. Jörg Lindemann
Department of Otorhinolaryngology, Head and Neck Surgery, University of Ulm, Frauensteige 12, 89075 Ulm, Germany, Tel: +49-731-500-59507, Fax: +49-731-500-59509
joerg.lindemann@uniklinik-ulm.de

***Please cite as***
*Keck T, Lindemann J. Numerical simulation and nasal air-conditioning. GMS Curr Top Otorhinolaryngol Head Neck Surg. 2010;9:Doc08.*
*DOI: 10.3205/cto000072, URN: urn:nbn:de:0183-cto0000729*

***This article is freely available from***
*http://www.egms.de/en/journals/cto/2011-9/cto000072.shtml*

***Published:*** *2011-04-27*